

Space-borne Atom Interferometric Gravitational Wave Detections: The Forecast of Bright Sirens on Cosmology

Rong-Gen Cai^{1,2,3,*} and Tao Yang^{4,†}

¹*CAS Key Laboratory of Theoretical Physics, Institute of Theoretical Physics, Chinese Academy of Sciences, Beijing 100190, China*

²*School of Physical Sciences, University of Chinese Academy of Sciences, No.19A Yuquan Road, Beijing 100049, China*

³*School of Fundamental Physics and Mathematical Sciences, Hangzhou Institute for Advanced Study (HIAS), University of Chinese Academy of Sciences, Hangzhou 310024, China*

⁴*Asia Pacific Center for Theoretical Physics, Pohang 37673, Korea*

(Dated: July 30, 2021)

Atom interferometers (AIs) as gravitational-wave (GW) detector had been proposed a decade ago. Both ground and space-based projects will be in construction and preparation in a near future. In this paper, for the first time, we investigate the potential of the space-borne AIs on detecting GW standard sirens and hence the applications on cosmology. We consider AEDGE as our fiducial AI GW detector and estimate the number of bright sirens that would be obtained within a 5-years data-taking period. We then construct the mock catalogue of bright sirens and predict their ability on constraining such as the Hubble constant, dynamics of dark energy, and modified gravity theory. The preliminary results show that there should be of order $\mathcal{O}(30)$ bright sirens detected within 5 years observation time by AEDGE. The bright sirens alone can measure H_0 with precision 2.1%, which is sufficient to arbitrate the Hubble tension. Combining current most precise electromagnetic experiments, the inclusion of AEDGE bright sirens can improve the measurement of equation of state of dark energy, though marginally. However, by modifying GW propagation on cosmological scales, the deviations from general relativity (modified gravity theory effects) can be constrained at 5.7% precision level, which is two times better than by 10-years operation of LIGO, Virgo and KAGRA network.

I. INTRODUCTION

The laser interferometer (LI) experiment of gravitational waves (GWs) conducted by LIGO/Virgo has achieved great success in the past five years. Up to now, LIGO has reported more than 50 confirmed GW events produced by the merger of the binary black holes (BBH), of the binary neutron stars (BNS), and of the neutron star-black hole binary (NS-BH) [1–5]. Especially, the first joint observation of GW from a BNS with its electromagnetic counterpart (EM) has opened the new era of multimessenger astronomy [2, 6, 7]. GWs as the novel signal play significant roles in modern cosmology, astrophysics and fundamental physics (see reviews [8–16], and a very recent review of the progress in GW physics [17]). In the next few years, the second generation ground-based GW detector network HLVKI (consisting of advanced LIGO-Hanford, advanced LIGO-Livingston, advanced Virgo, KAGRA and LIGO-India) will be in operation. On a longer timescale, around the 2030s the third-generation ground-based detectors such as Einstein Telescope (ET)¹ and Cosmic Explorer (CE)², and the space interferometer LISA³ will start to work. During the same time, Chinese space-based GW detectors like Taiji [18, 19] and

Tianqin [20] would also be launched. We expect a joint network of LI GW experiments from ground to space in the coming two decades.

For ground-based detectors typically their sensitive frequencies are $f > 10$ Hz, while for space-based experiments $f < 0.1$ Hz. Atom interferometers (AIs) are the candidates to probe GW in the Deci-Hz gap between LIGO/Virgo and LISA. The concept of AI GW detector has been proposed a decade ago [21–24]. The ground-based AI detector projects such as MAGIS [25] in US, ZAIGA [26] in China and AION [27] in UK are in preparation. The space-based AEDGE [28] has been proposed as a long-term plan.

AIs can be used as probes for both dark matter and gravitational waves (see the introductions in [25, 27, 28]). Several specific research of AIs such as the localization of GW sources [29] and the constraints of the deviations from general relativity (GR) [30] have been investigated. The GW frequency range of AIs between 0.01 and a few Hz is ideal for observation of mergers involving intermediate-mass black holes (IMBHs) with masses in the range 100 to 10^5 solar masses. However it can also observe the early stage of the inspiral of the BBH and BNS (see examples in [29, 30]). Take the space-borne AEDGE as an example, the motion of the detectors around the Sun as well as in Earth orbit would provide a very precise angular localization thus providing early warning of possible upcoming multimessenger events. There could be significant synergies between AEDGE measurements and observations in other frequency ranges by such as LISA, LIGO and ET.

* cairg@itp.ac.cn

† yangtao.lighink@gmail.com, corresponding author

¹ <http://www.et-gw.eu/>

² <https://cosmicexplorer.org/>

³ <https://www.lisamission.org/>

In this paper, to fill the gap in cosmological applications of AIs, we would like to investigate the potential of the standard sirens detected by AIs GW detector in cosmology and modified gravity theory. We focus on the bright sirens, i.e., BNS associated with a EM counterpart. The coincidence of GW and EM observations is the most straightforward way to obtain both the luminosity distance and redshift information thus constructing the $d_L - z$ relation for the cosmological constraint. We use the space-borne AEDGE as our default AI GW detector. The basic design of AEDGE requires two satellites operating along a single line-of-sight and separated by a long distance. The payload of each satellite will consist of cold atom technology as developed for state-of-the-art atom interferometry and atomic clocks [28]. This project assumes a minimum data-taking time of 3 years, which requires a mission duration of at least 5 years, while 10 years would be an ultimate goal. As a first step, we would like to see how many BNS and the joint GW+EM events can be detected by AEDGE in the future, and with these events how precisely one can measure the cosmological parameters such as the Hubble constant and constrain the feature of dark energy and deviations from GR.

The structure of this paper is as follows. In section II we construct the catalogue of the bright sirens by AEDGE in 5-years operation time and Hubble diagram is built accordingly. We then apply the mock bright sirens to several applications in cosmology in section III. We are pretty interested in the measurement of Hubble constant, the constraints of the dynamics of dark energy, and the modified gravity. Finally, we draw the conclusions and give some discussions in IV.

II. CONSTRUCTION OF BNS BRIGHT SIRENS

Following [31–33], we adopt the formation rate of massive binaries R_m by assuming an exponential time delay distribution $P(t_d, \tau) = \frac{1}{\tau} \exp(-t_d/\tau)$ with an e-fold time of $\tau = 100$ Myr [31],

$$R_m(z_m) = \int_{z_m}^{\infty} dz_f \frac{dt_f}{dz_f} R_f(z_f) P(t_d). \quad (1)$$

Here t_m (or the corresponding redshift z_m) and t_f are the look-back time when the systems merged and formed. $t_d = t_f - t_m$ is the time delay. R_f is the formation rate of massive binaries and we assume it is proportional to the Madau-Dickinson (MD) star formation rate [34],

$$\psi_{\text{MD}} = \psi_0 \frac{(1+z)^\alpha}{1 + [(1+z)/C]^\beta}, \quad (2)$$

with parameters $\alpha = 2.7$, $\beta = 5.6$ and $C = 2.9$. The coefficient ψ_0 is the normalization factor which is determined by the BNS rate we set at $z = 0$. We adopt $R_m(z = 0) = 920 \text{ Gpc}^{-3} \text{ yr}^{-1}$ which is the median rate estimated from the O1 and O2 LIGO/Virgo observation

run [3] and assume a Gaussian distribution of the mass of neutron stars. It is also consistent with the first half O3 run [4]. Then we can convert the merger rate per volume in the source frame to merger rate density per unit redshift in the observer frame

$$R_z(z) = \frac{R_m(z)}{1+z} \frac{dV(z)}{dz}, \quad (3)$$

where dV/dz is the comoving volume element.

Having the BNS merger rate $R_z(z)$ in Eq. 3, we can first sample of the BNS mergers from redshift 0 to 0.5 in a Monte-Carlo way. For every merger, we assign the sky location (θ, ϕ) and inclination angle ι from isotropic distribution. The polarization ψ , component masses of BNS are drawn from the uniform distribution, i.e., $\psi \in [0, 2\pi)$ and $m_1, m_2 \in [1, 2]M_\odot$. Then we can calculate the signal-to-noise ratio (SNR) in the inspiral phase

$$\rho^2 = \frac{5}{6} \frac{(G\mathcal{M}_c)^{5/3} \mathcal{F}^2}{c^3 \pi^4/3 d_L^2(z)} \int_{f_{\min}}^{f_{\max}} df \frac{f^{-7/3}}{S_n(f)}, \quad (4)$$

where $\mathcal{M}_c = (m_1 m_2)^{3/5} / (m_1 + m_2)^{1/5} (1+z)$ is the redshifted chirp mass. d_L is the luminosity distance. $S_n(f)$ is the one-sided noise power spectral density (PSD) of detector. The factor \mathcal{F} is to characterize the detector response, $\mathcal{F}^2 = \frac{(1+\cos^2 \iota)}{4} F_+^2 + \cos^2 \iota F_\times^2$. F_+ and F_\times are the antenna response functions to the + and \times polarizations of GW. For the bounds of the frequency in Eq. 4 we choose the lower and upper limits of the frequency to be the minimum and maximum sensitive frequency of AEDGE [28] since AEDGE's sensitive frequency mainly falls in the mid-frequency deciHz band, which is the early inspiral phase of the BNS.

To calculate the explicit form of the antenna response functions $F_+(t, \theta, \phi, \psi)$ and $F_\times(t, \theta, \phi, \psi)$, we follow [29] and consider the single-baseline detector AEDGE measuring the gravitational stretching and contraction along its baseline direction. Thus the detector response tensor D_{ij} from the baseline direction unit vector $a_i(t)$ is

$$D_{ij} = \frac{1}{2} a_i(t) a_j(t). \quad (5)$$

Then the GW strain tensor can be decomposed in terms of

$$h_{ij}(t) = h_+(t) e_{ij}^+ + h_\times(t) e_{ij}^\times, \quad (6)$$

here $e_{ij}^{+,\times}$ are the polarization tensors with $e_{ij}^+ = \hat{X}_i \hat{X}_j - \hat{Y}_i \hat{Y}_j$, and $e_{ij}^\times = \hat{X}_i \hat{Y}_j + \hat{Y}_i \hat{X}_j$. The basis is [35, 36],

$$\begin{aligned} \hat{X} = & (\sin \phi \cos \psi - \sin \psi \cos \phi \cos \theta, \\ & -\cos \phi \cos \psi - \sin \psi \sin \phi \cos \theta, \\ & \sin \psi \sin \theta), \end{aligned} \quad (7)$$

$$\begin{aligned} \hat{Y} = & (-\sin \phi \sin \psi - \cos \psi \cos \phi \cos \theta, \\ & \cos \phi \sin \psi - \cos \psi \sin \phi \cos \theta, \\ & \cos \psi \sin \theta). \end{aligned} \quad (8)$$

Then the observed waveform is given by

$$h(t) \equiv D_{ij} h_{ij} = h_+(t) F_+(t) + h_\times(t) F_\times(t), \quad (9)$$

with $F_+(t) = D_{ij}(t) e_{ij}^+$ and $F_\times(t) = D_{ij}(t) e_{ij}^\times$. Since the atom GW detector reorients and/or moves along the orbit around the Earth, the observed waveform and phase are modulated and Doppler-shifted, yielding important angular information. Without loss of generality, we can parameterize the detector location on the orbit by a unit vector $r_0(t) = (\cos \phi_a(t), \sin \phi_a(t), 0)$, where $\phi_a(t) = 2\pi t/T_{\text{AI}} + \phi_0$ is the azimuthal orbit angle around the Earth. T_{AI} is the AEDGE orbit period. The baseline direction of AEDGE is $a_0(t) = (-\sin \phi_a(t), \cos \phi_a(t), 0)$. Now we should transform the Earth polar coordinate of $r_0(t)$ and $a_0(t)$ to the Sun's polar coordinate as

$$r_{\text{AI}}(t) = \begin{pmatrix} \cos \phi_{\text{Ea}}(t) & -\sin \phi_{\text{Ea}}(t) & 0 \\ \sin \phi_{\text{Ea}}(t) & \cos \phi_{\text{Ea}}(t) & 0 \\ 0 & 0 & 1 \end{pmatrix} \cdot \begin{pmatrix} \cos \theta_{\text{inc}} & 0 & -\sin \theta_{\text{inc}} \\ 0 & 1 & 0 \\ \sin \theta_{\text{inc}} & 0 & \cos \theta_{\text{inc}} \end{pmatrix} \cdot r_0(t). \quad (10)$$

The baseline direction $a(t)$ is transformed similarly. The azimuthal angle of the Earth's orbit around the Sun is $\phi_{\text{Ea}} = 2\pi t/(1\text{yr}) + \phi_0'$. θ_{inc} is the inclination. We adopt a similar setup for AEDGE with MAGIS [25, 30], i.e., the detector consists of two satellites in identical circular geocentric orbits with an inclination $\theta_{\text{inc}} = 28.5^\circ$ at an altitude of 24×10^3 km and forming a baseline of 44×10^3 km with $T_{\text{AI}} = 10$ hours.

Now the derivation of the antenna response functions is straightforward. For every sampled BNS mergers we calculate the SNR from Eq. 4 and select the BNS GW events with a threshold $\text{SNR} > 8$. The histogram of the selected BNS GW events is shown in the left panel of Fig. 1, we can see within 5-years observation AEDGE can detect about 7819 BNS GW cases (1564/yr) from redshift 0–0.34, which can be compared to the second generation ground-based detector network HLVKI with 86/yr from redshift 0–0.15 [32, 33].

To use the BNS GWs as the bright sirens, we need to select the events with EM counterparts from these BNS GWs. We adopt the similar strategy as in [33] and consider the GW+EM counterpart as a temporal coincidence of the GW event with a short GRB. A GRB detected in coincidence with a GW signal requires that the peak flux is above the flux limit of the satellite. Considering the working time of AEDGE we select the THESEUS mission [37, 38] as the GRB satellite to predict the coincidences between GW events and GRBs. To calculate the probability of detecting a GRB counterpart, we first assume the Gaussian structured jet profile model for GRB

$$L(\theta_V) = L_c \exp\left(-\frac{\theta_V^2}{2\theta_c^2}\right), \quad (11)$$

here $L(\theta)$ is the luminosity per unit solid angle, θ_V is the viewing angle. L_c and θ_c are the structure parameters that define the sharpness of the angular profile. The structured jet parameter is given by $\theta_c = 4.7^\circ$ [39]. We then assume a standard broken power law form for the distribution of the short GRB

$$\Phi(L) \propto \begin{cases} (L/L_*)^a, & L < L_* \\ (L/L_*)^b, & L \geq L_* \end{cases} \quad (12)$$

where L is the isotropic rest frame luminosity in the 1–10000 keV energy range and L_* is a characteristic luminosity that separates the low and high end of the luminosity function and a and b are the characteristic slopes describing these regimes, respectively. We set $a = -1.95$, $b = -3$ and $L_* = 2 \times 10^{52}$ erg sec $^{-1}$ [40]. Now from the BNS GW candidates we can sample the GW+GRB events from the probability distribution $\Phi(L)dL$. The details of the calculation can be found in [33].

Figure 1 shows one realization of the GW detections and GW-GRB coincidences for 5-years observation of AEDGE assuming a GRB detector with the characteristics of THESEUS. The number of the useful bright sirens is drastically limited by the detections of GRB and only around 32 GW-GRB cases can be observed by THESEUS with its X-Gamma ray Imaging Spectrometer (XGIS). This result can be compared to HLVKI network with Fermi-GBM satellite for which only 14 GW-GRB cases can be detected in 10 years [32, 33].

Having the sampled GW-GRB candidates we can construct the Hubble diagram of future bright sirens by 5-years observation of AEDGE. We assume the fiducial cosmological model to be the Λ CDM model with $H_0 = 67.72$ km s $^{-1}$ Mpc $^{-1}$ and $\Omega_m = 0.3104$, corresponding to the mean values obtained from the latest *Planck* TT,TE,EE+lowE+lensing+BAO+Pantheon data combination [41]. We also fix the present CMB temperature $T_{\text{CMB}} = 2.7255$ K, the sum of neutrino masses $\Sigma_\nu m_\nu = 0.06$ eV, and the effective extra relativistic degrees of freedom $N_{\text{eff}} = 3.046$, as in the *Planck* baseline analysis. We assign three contributions to error of the luminosity distance, i.e., the instrumental error, the weak lensing and the peculiar velocity of the source galaxy. For weak lensing we adopt the analytically fitting formula [42, 43]

$$\left(\frac{\Delta d_L(z)}{d_L(z)}\right)_{\text{lens}} = 0.066 \left(\frac{1 - (1+z)^{-0.25}}{0.25}\right)^{1.8}. \quad (13)$$

We consider a delensing factor, i.e., the use of dedicated matter surveys along the line of sight of the GW event in order to estimate the lensing magnification distribution and thus remove part of the uncertainty due to weak lensing, which can reduce the weak lensing uncertainty. Following [44] we adopt a phenomenological formula

$$F_{\text{delens}}(z) = 1 - \frac{0.3}{\pi/2} \arctan(z/z_*), \quad (14)$$

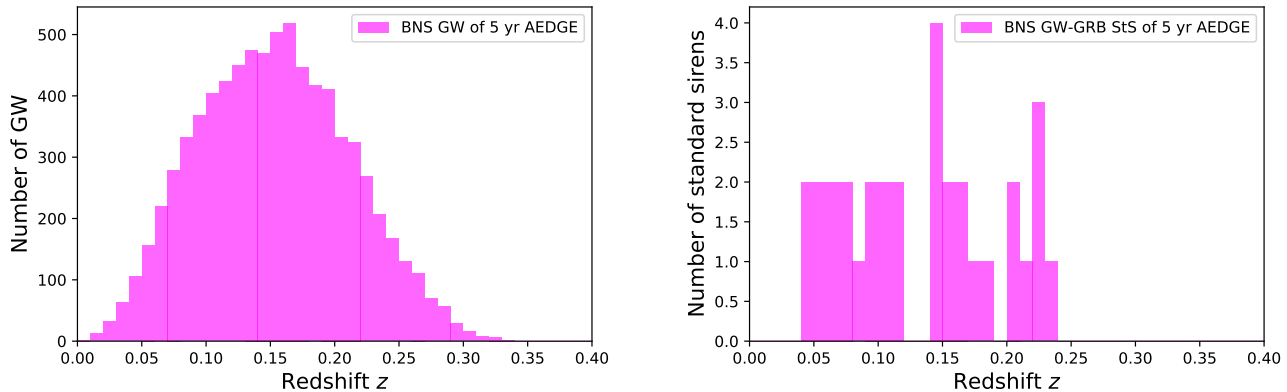


FIG. 1: A realization of the mock catalogue of 5 years detections of BNS GW (left) and GW-GRB standard sirens (StS) (right) from AEDGE assuming a GRB detector with the characteristics of THESEUS.

where $z_* = 0.073$. The final error from weak lensing is

$$\left(\frac{\Delta d_L(z)}{d_L(z)}\right)_{\text{delens}} = F_{\text{delens}}(z) \left(\frac{\Delta d_L(z)}{d_L(z)}\right)_{\text{lens}}. \quad (15)$$

For the peculiar velocity uncertainty, we use the fitting formula [45],

$$\left(\frac{\Delta d_L(z)}{d_L(z)}\right)_{\text{pec}} = \left[1 + \frac{c(1+z)^2}{H(z)d_L(z)}\right] \frac{\sqrt{\langle v^2 \rangle}}{c}, \quad (16)$$

here we set peculiar velocity value to be 500 km/s, in agreement with average values observed in galaxy catalogs. Finally the instrumental error due to the parameter estimation from the matched filtering waveform, is estimated as $\Delta d_L/d_L \sim 1/\text{SNR}$ [46, 47]. In this paper we consider the BNS associated with a short GRB which is usually beamed within an angle of about 25° . The correlation between distance and inclination is substantially broken, so the above estimate becomes accurate [35]. The final uncertainty of the luminosity distance is just the sum of the above errors in quadrature. We construct the Hubble diagram of bright sirens from future AEDGE in Fig. 2.

III. COSMOLOGICAL APPLICATIONS

Gravitational waves as the standard sirens have many applications in cosmology. In this paper we focus on using bright sirens to measure the Hubble constant, constraining the dynamics of dark energy, and testing the validity of GR. To measure the cosmological parameters, StS is very analogous to the SNe Ia as the standard candles. The $d_L - z$ relation of standard sirens does not rely on the calibration and the underlying physics is very clear, which is the great advantages over SNe Ia. This feature of StS makes it a perfect probe of the expansion of our Universe and hence to measure the cosmological

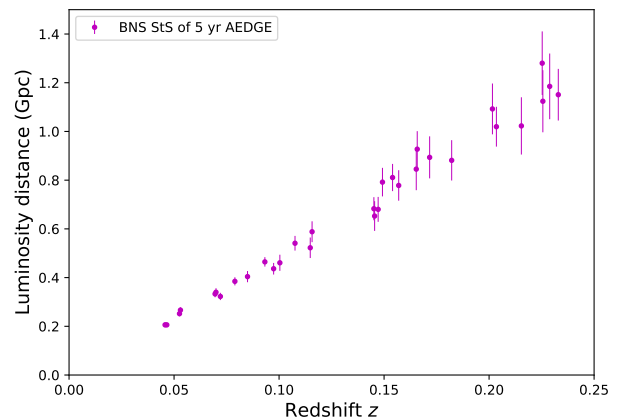


FIG. 2: The Hubble diagram of one realization of mock bright sirens from AEDGE.

parameters especially for Hubble constant and equation of state of dark energy. On the other hand, StS is very sensitive to the propagation of GW when considering the modified gravity theories. So that we can test GR from the propagation of GWs across cosmological distances [32, 48–62]. In a general modified gravity theory the linearized evolution equation for GWs traveling on an FRW background is [53]

$$\tilde{h}''_A + 2[1 - \delta(\eta)]\mathcal{H}\tilde{h}'_A + [c_T^2(\eta)k^2 + m_T^2(\eta)]\tilde{h}_A = \Pi_A, \quad (17)$$

\tilde{h}_A are the Fourier modes of the GW amplitude and $A = +, \times$ labels the two polarizations. $\mathcal{H} = a'/a$ is the Hubble parameter in conformal time and the primes indicating derivatives with respect to conformal time η . The function $\delta(\eta)$ is introduced to modify the friction term in the propagation equation, thus denoting the effects of modified gravity theory. c_T corresponds to the speed of gravitational waves. In theories of modified gravity the

tensor mode can be massive, with m_T its mass. In GR we have $\delta = 0$, $c_T = c$, and $m_T = 0$. The detection of GW170817/GRB170817A puts a very tight constraint $(c_T - c)/c < \mathcal{O}(10^{-15})$ [7]. In this paper we only consider the extra δ in the friction term. Then it is possible to show that standard sirens do not measure the usual electromagnetic luminosity distance but a gravitational-wave luminosity distance [48, 49],

$$d_L^{\text{gw}}(z) = d_L^{\text{em}}(z) \exp \left\{ - \int_0^z \frac{dz'}{1+z'} \delta(z') \right\}. \quad (18)$$

We can use the the difference between $d_L^{\text{gw}}(z)$ and $d_L^{\text{em}}(z)$ as a smoking gun of the modified gravity theories.

Now we can apply the mock bright sirens by AEDGE to some cosmological applications. As in [33] we consider four parameterizations for dark energy model and/or modified gravity theory as follows:

- We assume the baseline Λ CDM model with a cosmological constant ($w = -1$). We would like to investigate how precisely the bright sirens of AEDGE can constrain the Hubble constant H_0 and the dark matter density parameter Ω_m .
- We extend the baseline Λ CDM model and assume a constant equation of state of dark energy w , which is denoted as w CDM.
- We consider further the dynamics of dark energy and assume a Chevallier-Polarski-Linder (CPL) form $w(z) = w_0 + w_a z/(1+z)$ for the equation of state [63].
- We assume a phenomenological parameterization of the modified GW propagation $\Xi(z) \equiv d_L^{\text{gw}}(z)/d_L^{\text{em}}(z) = \Xi_0 + (1 - \Xi_0)/(1+z)^n$, which is denoted as MG.

We also include the traditional EM data sets as comparison. We use the CMB data from latest *Planck* [41]. For BAO we adopt the isotropic constraints provided by 6dFGS at $z_{\text{eff}} = 0.106$ [64], SDSS-MGS DR7 at $z_{\text{eff}} = 0.15$ [65], and ‘‘consensus’’ BAOs in three redshift slices with effective redshifts $z_{\text{eff}} = 0.38, 0.51, \text{ and } 0.61$ [66–68]. We use the Pantheon data [69] as the latest compilation of SNe Ia. For every models we consider different data sets combinations, i.e., AEDGE standard sirens alone, *Planck*+BAO+Pantheon, and finally all together. To get the posteriors of these cosmological parameters, we run Markov-Chain Monte-Carlo (MCMC) by the package COBAYA [70, 71]. The marginalized statistics of the parameters and the plots are produced by the Python package GETDIST [72]. The contour plots of the cosmological parameters are shown in Fig. 3. Note that we just show the constraints of the important parameters in every models. The detailed result for every parameters is shown in Tab. I.

IV. CONCLUSION AND DISCUSSIONS

In this paper, for the first time, we consider the atom interferometer as a novel GW detector and investigate its potential to detect bright sirens and hence the applications on cosmology and modified gravity theory. We choose the space-borne AEDGE as our fiducial AI detector and assume a five-years data-taking period. Based on current knowledge of the BNS merger rates and GRB model, we estimate the number of bright sirens that AEDGE will detect within five years in the future. We then apply these bright sirens to several cosmological applications, such as the measurement of Hubble constant, the constraint of dynamics of dark energy and the deviations from GR.

As a preliminary investigation, our results show there should be around 32 bright siren detections within 5 years observation time by AEDGE. Though about 7819 BNS cases should be observed, the joint GW-GRB events are drastically limited by the EM counterpart detectability. Note we only consider GRB as the EM counterpart in this paper. By these 32 bright sirens alone, Hubble constant can be measured with a precision of 2.1%, which is sufficient to arbitrate the current tension between local and high- z measurements of H_0 [73]. While it requires more than 50 events for this level of precision by HLV (LIGO+Virgo) network [73]. Adding AEDGE to current *Planck*+BAO+Pantheon datasets we can improve the measurement of H_0 from 0.6% to 0.5%. For the dynamics of dark energy, AEDGE itself can not put a tight constraint for the equation of state. This is due to the number and redshift range (only up to 0.25) of the events. However, the inclusion of AEDGE will still improve the constraints of w and w_a though marginally. When constraining the MG effects from the propagation of GW, AEDGE 5-years bright sirens with current most precise EM experiments can measure Ξ_0 at 5.7% precision level, which is two times better than by 10-years operation of HLVKI network [32].

In addition to BNS bright sirens, MBHBs are also accompanied by the EM counterpart and they are the main targets of LISA [43, 74]. We have also done the simulations of MBHBs observed by AEDGE. However, only very late pre-merger stage can enter the frequency band of AEDGE. From the calculation of fisher matrix, the uncertainties of the waveform parameters including the luminosity distance and that related to the localization are very large, which makes it impossible to apply the MBHBs standard sirens in this paper.

Though the number of BNS bright sirens is very limited, the dark sirens including BNS, BBH without EM counterparts should provide us with a huge amounts of cases. From the fisher matrix calculation, we have checked that the precision of the sky localization of BNS and BBH source measured by AEDGE is much higher than LI detectors (like LIGO and ET). This is due to the fact that from AEDGE we can observe the BNS and BBH systems in the inspiral stage for a long time before

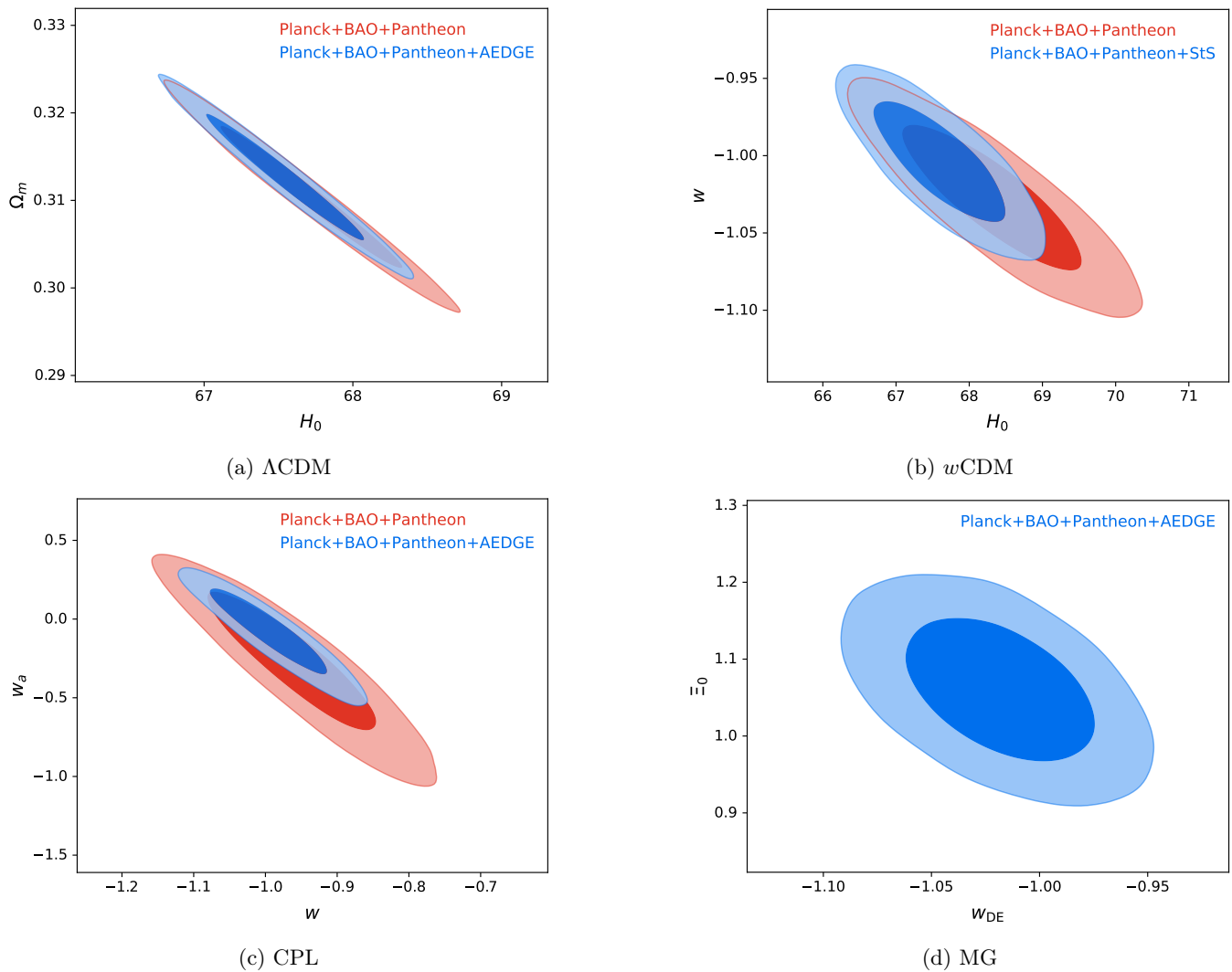


FIG. 3: The constraints of the selected parameters in every DE/MG models. Contours contain 68 % and 95 % of the probability.

they merge. Also the single baseline orbits around the Earth and the Sun, causing it to reorient and change position significantly during the lifetime of the source, and making it similar to having multiple baselines/detectors, thus more angular information would be encoded [29]. We can anticipate a decent estimation of the redshift in a statistical method. We leave this for future research.

ACKNOWLEDGMENTS

The authors would like to thank Ling-Feng Wang, Wen-Hong Ruan and Chang Liu for helpful discussion on the fisher matrix calculation. RGC is sup-

ported by the National Natural Science Foundation of China Grants No.11690022, No.11821505, No.11991052, No.11947302 and by the Strategic Priority Research Program of the Chinese Academy of Sciences Grant No.XDB23030100, the Key Research Program of the CAS Grant No.XDPB15, and the Key Research Program of FrontierSciences of CAS. TY would like to thank the secondment between APCTP and ITP in May and June for the completion of this work. This work is supported by an appointment to the YST Program at the APCTP through the Science and Technology Promotion Fund and Lottery Fund of the Korean Government, and the Korean Local Governments - Gyeongsangbuk-do Province and Pohang City.

[1] B. P. Abbott *et al.* (LIGO Scientific, Virgo), *Phys. Rev. Lett.* **116**, 061102 (2016), arXiv:1602.03837 [gr-qc].

[2] B. P. Abbott *et al.* (LIGO Scientific, Virgo), *Phys. Rev.*

| Data and model | Parameter | H_0 | Ω_m | w_0 | w_a | Ξ_0 |
|---------------------------|---------------|----------------------|------------------------|----------------------|-------------------------|-------------------|
| AEDGE | Λ CDM | 66.2 ± 1.4 | $0.46^{+0.22}_{-0.30}$ | – | – | – |
| | w CDM | $66.0^{+1.6}_{-2.1}$ | $0.61^{+0.35}_{-0.33}$ | $-1.5^{+1.4}_{-1.2}$ | – | – |
| | CPL | $66.1^{+1.6}_{-2.0}$ | $0.59^{+0.33}_{-0.16}$ | $-1.6^{+1.4}_{-1.3}$ | – | – |
| Planck+BAO+Pantheon | Λ CDM | 67.72 ± 0.40 | 0.3104 ± 0.0054 | – | – | – |
| | w CDM | 68.34 ± 0.81 | 0.3057 ± 0.0075 | -1.028 ± 0.031 | – | – |
| Planck+BAO+Pantheon+AEDGE | CPL | 68.31 ± 0.82 | 0.3065 ± 0.0077 | -0.957 ± 0.080 | $-0.29^{+0.32}_{-0.26}$ | – |
| | Λ CDM | 67.55 ± 0.35 | 0.3126 ± 0.0047 | – | – | – |
| | w CDM | 67.61 ± 0.59 | 0.3123 ± 0.0057 | -1.004 ± 0.026 | – | – |
| Planck+BAO+Pantheon+AEDGE | CPL | 67.50 ± 0.61 | 0.3138 ± 0.0061 | -0.944 ± 0.075 | $-0.23^{+0.29}_{-0.25}$ | – |
| | MG | 68.07 ± 0.74 | 0.3081 ± 0.0070 | -1.019 ± 0.029 | – | 1.061 ± 0.061 |

TABLE I: The constraints of the parameters in every DE/MG models for different data sets combinations. The numbers are the mean values with 68% limits of the errors.

- Lett.* **119**, 161101 (2017), [arXiv:1710.05832 \[gr-qc\]](#).
- [3] B. P. Abbott *et al.* (LIGO Scientific, Virgo), *Phys. Rev. X* **9**, 031040 (2019), [arXiv:1811.12907 \[astro-ph.HE\]](#).
- [4] R. Abbott *et al.* (LIGO Scientific, Virgo), *Phys. Rev. X* **11**, 021053 (2021), [arXiv:2010.14527 \[gr-qc\]](#).
- [5] R. Abbott *et al.* (LIGO Scientific, KAGRA, VIRGO), *Astrophys. J. Lett.* **915**, L5 (2021), [arXiv:2106.15163 \[astro-ph.HE\]](#).
- [6] B. P. Abbott *et al.* (LIGO Scientific, Virgo, Fermi GBM, INTEGRAL, IceCube, AstroSat Cadmium Zinc Telluride Imager Team, IPN, Insight-Hxmt, ANTARES, Swift, AGILE Team, 1M2H Team, Dark Energy Camera GW-EM, DES, DLT40, GRAWITA, Fermi-LAT, ATCA, ASKAP, Las Cumbres Observatory Group, OzGrav, DWF (Deeper Wider Faster Program), AST3, CAAS-TRO, VINROUGE, MASTER, J-GEM, GROWTH, JAGWAR, CaltechNRAO, TTU-NRAO, NuSTAR, Pan-STARRS, MAXI Team, TZAC Consortium, KU, Nordic Optical Telescope, ePESSTO, GROND, Texas Tech University, SALT Group, TOROS, BOOTES, MWA, CALET, IKI-GW Follow-up, H.E.S.S., LOFAR, LWA, HAWC, Pierre Auger, ALMA, Euro VLBI Team, Pi of Sky, Chandra Team at McGill University, DFN, ATLAS Telescopes, High Time Resolution Universe Survey, RIMAS, RATIR, SKA South Africa/MeerKAT), *Astrophys. J. Lett.* **848**, L12 (2017), [arXiv:1710.05833 \[astro-ph.HE\]](#).
- [7] B. P. Abbott *et al.* (LIGO Scientific, Virgo, Fermi-GBM, INTEGRAL), *Astrophys. J. Lett.* **848**, L13 (2017), [arXiv:1710.05834 \[astro-ph.HE\]](#).
- [8] B. F. Schutz, *Class. Quant. Grav.* **16**, A131 (1999), [arXiv:gr-qc/9911034](#).
- [9] L. Barack *et al.*, *Class. Quant. Grav.* **36**, 143001 (2019), [arXiv:1806.05195 \[gr-qc\]](#).
- [10] M. Sasaki, T. Suyama, T. Tanaka, and S. Yokoyama, *Class. Quant. Grav.* **35**, 063001 (2018), [arXiv:1801.05235 \[astro-ph.CO\]](#).
- [11] J. R. Gair, M. Vallisneri, S. L. Larson, and J. G. Baker, *Living Rev. Rel.* **16**, 7 (2013), [arXiv:1212.5575 \[gr-qc\]](#).
- [12] J. M. Ezquiaga and M. Zumalacárregui, *Front. Astron. Space Sci.* **5**, 44 (2018), [arXiv:1807.09241 \[astro-ph.CO\]](#).
- [13] R.-G. Cai, Z. Cao, Z.-K. Guo, S.-J. Wang, and T. Yang, *Natl. Sci. Rev.* **4**, 687 (2017), [arXiv:1703.00187 \[gr-qc\]](#).
- [14] P. Mészáros, D. B. Fox, C. Hanna, and K. Murase, *Nature Rev. Phys.* **1**, 585 (2019), [arXiv:1906.10212 \[astro-ph.HE\]](#).
- [15] N. Christensen, *Rept. Prog. Phys.* **82**, 016903 (2019), [arXiv:1811.08797 \[gr-qc\]](#).
- [16] S. E. Perkins, N. Yunes, and E. Berti, *Phys. Rev. D* **103**, 044024 (2021), [arXiv:2010.09010 \[gr-qc\]](#).
- [17] L. Bian *et al.*, (2021), [arXiv:2106.10235 \[gr-qc\]](#).
- [18] W.-R. Hu and Y.-L. Wu, *Natl. Sci. Rev.* **4**, 685 (2017).
- [19] W.-H. Ruan, Z.-K. Guo, R.-G. Cai, and Y.-Z. Zhang, *Int. J. Mod. Phys. A* **35**, 2050075 (2020), [arXiv:1807.09495 \[gr-qc\]](#).
- [20] J. Luo *et al.* (TianQin), *Class. Quant. Grav.* **33**, 035010 (2016), [arXiv:1512.02076 \[astro-ph.IM\]](#).
- [21] S. Dimopoulos, P. W. Graham, J. M. Hogan, M. A. Kasevich, and S. Rajendran, *Phys. Lett. B* **678**, 37 (2009), [arXiv:0712.1250 \[gr-qc\]](#).
- [22] S. Dimopoulos, P. W. Graham, J. M. Hogan, M. A. Kasevich, and S. Rajendran, *Phys. Rev. D* **78**, 122002 (2008), [arXiv:0806.2125 \[gr-qc\]](#).
- [23] P. W. Graham, J. M. Hogan, M. A. Kasevich, and S. Rajendran, *Phys. Rev. Lett.* **110**, 171102 (2013), [arXiv:1206.0818 \[quant-ph\]](#).
- [24] J. M. Hogan and M. A. Kasevich, *Phys. Rev. A* **94**, 033632 (2016), [arXiv:1501.06797 \[physics.atom-ph\]](#).
- [25] P. W. Graham, J. M. Hogan, M. A. Kasevich, S. Rajendran, and R. W. Romani (MAGIS), (2017), [arXiv:1711.02225 \[astro-ph.IM\]](#).
- [26] M.-S. Zhan *et al.*, *Int. J. Mod. Phys. D* **29**, 1940005 (2019), [arXiv:1903.09288 \[physics.atom-ph\]](#).
- [27] L. Badurina *et al.*, *JCAP* **05**, 011 (2020), [arXiv:1911.11755 \[astro-ph.CO\]](#).
- [28] Y. A. El-Neaj *et al.* (AEDGE), *EPJ Quant. Technol.* **7**, 6 (2020), [arXiv:1908.00802 \[gr-qc\]](#).
- [29] P. W. Graham and S. Jung, *Phys. Rev. D* **97**, 024052 (2018), [arXiv:1710.03269 \[gr-qc\]](#).
- [30] J. Ellis and V. Vaskonen, *Phys. Rev. D* **101**, 124013 (2020), [arXiv:2003.13480 \[gr-qc\]](#).
- [31] S. Vitale, W. M. Farr, K. Ng, and C. L. Rodriguez, *Astrophys. J. Lett.* **886**, L1 (2019), [arXiv:1808.00901 \[astro-ph.HE\]](#).
- [32] E. Belgacem, Y. Dirian, S. Foffa, E. J. Howell, M. Maggiore, and T. Regimbau, *JCAP* **08**, 015 (2019), [arXiv:1907.01487 \[astro-ph.CO\]](#).
- [33] T. Yang, *JCAP* **05**, 044 (2021), [arXiv:2103.01923 \[astro-ph.CO\]](#).
- [34] P. Madau and M. Dickinson, *Ann. Rev. Astron. Astrophys.* **52**, 415 (2014), [arXiv:1403.0007 \[astro-ph.CO\]](#).
- [35] S. Nissanke, D. E. Holz, S. A. Hughes, N. Dalal, and J. L. Sievers, *Astrophys. J.* **725**, 496 (2010), [arXiv:0904.1017 \[astro-ph.CO\]](#).

- [36] C. Cutler and E. E. Flanagan, *Phys. Rev. D* **49**, 2658 (1994), [arXiv:gr-qc/9402014](#).
- [37] L. Amati *et al.* (THESEUS), *Adv. Space Res.* **62**, 191 (2018), [arXiv:1710.04638 \[astro-ph.IM\]](#).
- [38] G. Stratta *et al.* (THESEUS), *Adv. Space Res.* **62**, 662 (2018), [arXiv:1712.08153 \[astro-ph.HE\]](#).
- [39] E. J. Howell, K. Ackley, A. Rowlinson, and D. Coward, (2018), [10.1093/mnras/stz455](#), [arXiv:1811.09168 \[astro-ph.HE\]](#).
- [40] D. Wanderman and T. Piran, *Mon. Not. Roy. Astron. Soc.* **448**, 3026 (2015), [arXiv:1405.5878 \[astro-ph.HE\]](#).
- [41] N. Aghanim *et al.* (Planck), *Astron. Astrophys.* **641**, A6 (2020), [arXiv:1807.06209 \[astro-ph.CO\]](#).
- [42] C. M. Hirata, D. E. Holz, and C. Cutler, *Phys. Rev. D* **81**, 124046 (2010), [arXiv:1004.3988 \[astro-ph.CO\]](#).
- [43] N. Tamanini, C. Caprini, E. Barausse, A. Sesana, A. Klein, and A. Petiteau, *JCAP* **04**, 002 (2016), [arXiv:1601.07112 \[astro-ph.CO\]](#).
- [44] L. Speri, N. Tamanini, R. R. Caldwell, J. R. Gair, and B. Wang, *Phys. Rev. D* **103**, 083526 (2021), [arXiv:2010.09049 \[astro-ph.CO\]](#).
- [45] B. Kocsis, Z. Frei, Z. Haiman, and K. Menou, *Astrophys. J.* **637**, 27 (2006), [arXiv:astro-ph/0505394](#).
- [46] N. Dalal, D. E. Holz, S. A. Hughes, and B. Jain, *Phys. Rev. D* **74**, 063006 (2006), [arXiv:astro-ph/0601275](#).
- [47] T. G. F. Li, *Extracting Physics from Gravitational Waves: Testing the Strong-field Dynamics of General Relativity and Inferring the Large-scale Structure of the Universe*, Ph.D. thesis, Vrije U., Amsterdam (2013).
- [48] E. Belgacem, Y. Dirian, S. Foffa, and M. Maggiore, *Phys. Rev. D* **97**, 104066 (2018), [arXiv:1712.08108 \[astro-ph.CO\]](#).
- [49] E. Belgacem, Y. Dirian, S. Foffa, and M. Maggiore, *Phys. Rev. D* **98**, 023510 (2018), [arXiv:1805.08731 \[gr-qc\]](#).
- [50] A. Nishizawa, *Phys. Rev. D* **97**, 104037 (2018), [arXiv:1710.04825 \[gr-qc\]](#).
- [51] S. Arai and A. Nishizawa, *Phys. Rev. D* **97**, 104038 (2018), [arXiv:1711.03776 \[gr-qc\]](#).
- [52] A. Nishizawa and S. Arai, *Phys. Rev. D* **99**, 104038 (2019), [arXiv:1901.08249 \[gr-qc\]](#).
- [53] E. Belgacem *et al.* (LISA Cosmology Working Group), *JCAP* **07**, 024 (2019), [arXiv:1906.01593 \[astro-ph.CO\]](#).
- [54] E. Belgacem, S. Foffa, M. Maggiore, and T. Yang, *Phys. Rev. D* **101**, 063505 (2020), [arXiv:1911.11497 \[astro-ph.CO\]](#).
- [55] S. Mukherjee, B. D. Wandelt, and J. Silk, *Mon. Not. Roy. Astron. Soc.* **494**, 1956 (2020), [arXiv:1908.08951 \[astro-ph.CO\]](#).
- [56] R. D’Agostino and R. C. Nunes, *Phys. Rev. D* **100**, 044041 (2019), [arXiv:1907.05516 \[gr-qc\]](#).
- [57] A. Bonilla, R. D’Agostino, R. C. Nunes, and J. C. N. de Araujo, *JCAP* **03**, 015 (2020), [arXiv:1910.05631 \[gr-qc\]](#).
- [58] S. Mukherjee, B. D. Wandelt, and J. Silk, *Mon. Not. Roy. Astron. Soc.* **502**, 1136 (2021), [arXiv:2012.15316 \[astro-ph.CO\]](#).
- [59] M. Kalomenopoulos, S. Khochfar, J. Gair, and S. Arai, *Mon. Not. Roy. Astron. Soc.* **503**, 3179 (2021), [arXiv:2007.15020 \[astro-ph.CO\]](#).
- [60] S. Mastrogiovanni, L. Haegel, C. Karathanasis, I. M. n. Hernandez, and D. A. Steer, *JCAP* **02**, 043 (2021), [arXiv:2010.04047 \[gr-qc\]](#).
- [61] S. Mastrogiovanni, D. Steer, and M. Barsuglia, *Phys. Rev. D* **102**, 044009 (2020), [arXiv:2004.01632 \[gr-qc\]](#).
- [62] A. Finke, S. Foffa, F. Iacovelli, M. Maggiore, and M. Mancarella, (2021), [arXiv:2101.12660 \[astro-ph.CO\]](#).
- [63] M. Chevallier and D. Polarski, *Int. J. Mod. Phys. D* **10**, 213 (2001), [arXiv:gr-qc/0009008](#).
- [64] F. Beutler, C. Blake, M. Colless, D. H. Jones, L. Staveley-Smith, L. Campbell, Q. Parker, W. Saunders, and F. Watson, *Mon. Not. Roy. Astron. Soc.* **416**, 3017 (2011), [arXiv:1106.3366 \[astro-ph.CO\]](#).
- [65] A. J. Ross, L. Samushia, C. Howlett, W. J. Percival, A. Burden, and M. Manera, *Mon. Not. Roy. Astron. Soc.* **449**, 835 (2015), [arXiv:1409.3242 \[astro-ph.CO\]](#).
- [66] A. J. Ross *et al.* (BOSS), *Mon. Not. Roy. Astron. Soc.* **464**, 1168 (2017), [arXiv:1607.03145 \[astro-ph.CO\]](#).
- [67] M. Vargas-Magaña *et al.*, *Mon. Not. Roy. Astron. Soc.* **477**, 1153 (2018), [arXiv:1610.03506 \[astro-ph.CO\]](#).
- [68] F. Beutler *et al.* (BOSS), *Mon. Not. Roy. Astron. Soc.* **464**, 3409 (2017), [arXiv:1607.03149 \[astro-ph.CO\]](#).
- [69] D. M. Scolnic *et al.*, *Astrophys. J.* **859**, 101 (2018), [arXiv:1710.00845 \[astro-ph.CO\]](#).
- [70] J. Torrado and A. Lewis, *JCAP* **05**, 057 (2021), [arXiv:2005.05290 \[astro-ph.IM\]](#).
- [71] J. Torrado and A. Lewis, “Cobaya: Bayesian analysis in cosmology,” (2019), [ascl:1910.019](#).
- [72] A. Lewis, (2019), [arXiv:1910.13970 \[astro-ph.IM\]](#).
- [73] H.-Y. Chen, M. Fishbach, and D. E. Holz, *Nature* **562**, 545 (2018), [arXiv:1712.06531 \[astro-ph.CO\]](#).
- [74] A. Klein *et al.*, *Phys. Rev. D* **93**, 024003 (2016), [arXiv:1511.05581 \[gr-qc\]](#).